2015 International Symposium on Nonlinear Theory and its Applications
NOLTA2015, Kowloon, Hong Kong, China, December 1-4, 2015

Stabilization of Unstable Quasi-Periodic Solutions in Asymmetric Chaotic Neural Network Circuits — Numerical simulations and circuit experiments —

Masahiro OGAWA[†], Yoshihiko HORIO[†], Natsuhiro ICHINOSE[††], and Motomasa KOMURO[†††]

[†]Graduate School of Engineering, Tokyo Denki University
5 Senju Asahi-cho, Adachi-ku, Tokyo 120-8551, Japan
[††]Graduate School of Informatics, Kyoto University
36-1 Yoshida-Hommachi, Sakyo-ku, Kyoto, 606-8501, Japan
[†††]Center for Fundamental Education, Teikyo University of Science
2525 Yatsusawa, Uenohara-shi, Yamanashi, 409-0193, Japan
[†]Email: 14kme07@ms.dendai.ac.jp

1. Abstract

We, first, experimentally stabilize a quasi-periodic orbit in a switched-capacitor asymmetric 3-neuron chaotic neural network (CNN) circuit through a pole-placement control. The test method for quasi-periodicity suitable for noisy data is used to confirm the results. Second, we extend the 3-neuron CNN to a 5-neuron CNN. From the numerical simulations, we confirm the effectiveness of the control procedure to stabilize an unstable quasi-periodic orbit in the 5-neuron CNN.

2. Introduction

Chaos controls aim at stabilization of an inherent unstable periodic orbit in the chaotic attractor. An example of such chaos control methods is the OGY method proposed by Ott, Grebogi, and Yorke [1]. Another example is the delayed feedback control method proposed by Pyragas [2]. Unlike these chaos controls, Ichinose et al. proposed a method to stabilize an unstable quasi-periodic orbit instead of the periodic one [3][4].

They demonstrated the stabilization of the unstable quasi-periodic solution using the pole placement method [5] in an asymmetric chaotic neural network (CNN) [6] through numerical simulations. However, the effectiveness of the proposed method has not been confirmed by physical experiments. In [7], we constructed the asymmetric CNN with 3 chaotic neurons using a switched-capacitor circuit technique in order to experimentally observe the stabilization of the quasi-periodic orbit. The experimental results confirmed that the stabilization technique is effective in real systems with noise and mismatches among circuits elements.

In this paper, we first continue the circuit experiments with the 3-neuron CNN with different set of the parameter values from that in [7]. Second, we extend the 3-neuron CNN to a 5-neuron asymmetric CNN. Then, we confirm the stabilization of the quasi-periodic orbits through numerical simulations.

3. Stabilization of an unstable quasi-periodic solution in the asymmetric CNN

The chaotic neural network (CNN) used below is based on the chaotic neural network model proposed in [6], but we introduce an asymmetric mutual connections among neurons. The asymmetric CNN with 3 chaotic neurons [7] is defined as

$$x_1(n+1) = kx_1(n) - (\alpha-\beta)y_1(n) + a - \frac{\beta+d}{2}y_3(n) - \frac{\beta-d}{2}y_2(n) + F\cdot u(n), \quad (1)$$

$$x_2(n+1) = kx_2(n) - (\alpha-\beta)y_2(n) + a - \frac{\beta+d}{2}y_1(n) - \frac{\beta-d}{2}y_3(n) + F\cdot u(n), \quad (2)$$

$$x_3(n+1) = kx_3(n) - (\alpha-\beta)y_3(n) + a - \frac{\beta+d}{2}y_2(n) - \frac{\beta-d}{2}y_1(n) + F\cdot u(n), \quad (3)$$

where $x_i(n)$ $(i = 1, 2, 3)$ is the internal state of the neuron i at discrete time n, $y_i(n) = f(x_i(n))$ is the output of the neuron i, k is a refractory decay constant, α is a scaling parameter of the refractoriness, a is an external input, β is the basic coupling strength, d introduces the asymmetric connection strength, $u(n)$ is a control input, and F is a control gain.

The output function $f(\cdot)$ is sigmoidal and given by

$$f(x) = \frac{1}{1+e^{-x/\varepsilon}}, \quad (4)$$

where ε gives the steepness of the function. When $u(n) = 0$, i.e., without control, the CNN given by Eq. (1) to Eq. (3), has a complete synchronized solution of $x_1(n) = x_2(n) = x_3(n)$ by certain values of parameters. In this case, the behavior of the CNN can be reduced to that of a single neuron as

$$x_1(n+1) = kx_1(n) - \alpha y_1(n) + a. \quad (5)$$

Therefore, the fixed point x^*, if exist, of the CNN satisfies $x^* = kx^* - \alpha f(x^*) + a$. Defining $\gamma = f'(x^*)$ and solve for x^* yields

$$x^* = -\epsilon \log \frac{1 - 2\epsilon\gamma \pm \sqrt{1-4\epsilon\gamma}}{2\epsilon\gamma}. \quad (6)$$

Therefore, the completely synchronized CNN has the fixed point of $x^* = x_1(n) = x_2(n) = x_3(n)$, which is referred to as the complete synchronization fixed point.

With the eigenvalues of the Jacobian matrix J at x^* given by Eq. (7), we can examine the stability of x^*.

$$\lambda_1 = k - \alpha\gamma,\ \lambda_{2,3} = k - \left(\alpha - \frac{3}{2}\beta\right)\gamma \pm i\frac{\sqrt{3}}{2}d\gamma. \quad (7)$$

The real eigenvalue λ_1 corresponds to the synchronous direction of the eigenvector. On the other hand, the complex eigenvalues λ_2 and λ_3 give the asynchronous direction of the eigenvector, which contribute to desynchronization. By destabilizing λ_2 and λ_3 while keeping λ_1 stable, the fixed point x^* will bifurcate to a stable quasi-periodic solution. In order to realize the bifurcation of x^* to the quasi-periodic solution, we use the state-feedback control method based on a pole-placement technique [5].

The bifurcation diagram of $x_1(n)$ when we change the value of a is shown Fig. 1(a). The parameter values of $k = 0.7$, $\alpha = 1$, $\varepsilon = 0.05$, $\beta = 2/3$, and $d = 0.3$ were used to obtain the figure. In Fig. 1(a), the dashed-line indicates the point where $a = 0.059776$. When $a > 0.059776$, $|\lambda_1| > 1$ (unstable); as a result, a period-doubling bifurcation occurs. In addition, the solid line in Fig. 1(a) shows the point where $a = 0.140223$. When $a > 0.140223$, λ_2 and λ_3 become unstable because $|\lambda_{2,3}| > 1$. As a result, an unstable quasi-periodic solution occurs by the Neimark-Sacker bifurcation. In this case, a synchronized chaotic solution is stabilized.

Next, we replace λ_1 with a stable λ' by the state feedback technique with pole placement method [9], using the additional feedback input $u(n)$ given by

$$u(n) = y_1(n) + y_2(n) + y_3(n) - 3f(x^*). \quad (8)$$

In this case, the feedback gain can be set as

$$F = \frac{\lambda' - k + \alpha\gamma}{3\gamma}. \quad (9)$$

The bifurcation diagram of $x_1(n)$ when we change a is shown in Fig. 1(b) with $\lambda' = -0.9$, $k = 0.7$, $\alpha = 1$, $\varepsilon = 0.05$, $\beta = 2/3$, and $d = 0.3$. As shown in Fig. 1(b), λ_1 does not bifurcate even if the value of a passes the dashed-line $\boxed{1}$, which corresponds to the case where $|\lambda_1| > 1$ in Fig. 1(a). On the other hand, when the value of a crosses the line $\boxed{2}$, a quasi-periodic solution is generated because $|\lambda_{2,3}| > 1$.

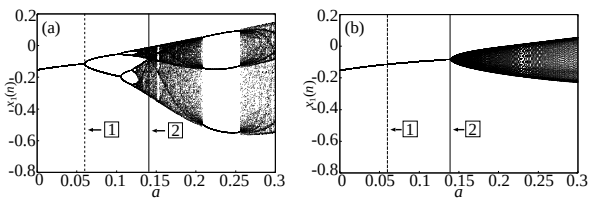

Figure 1: The bifurcation diagram of $x_1(n)$ when we swept a, (a) without, and (b) with the feedback control. ((a) and (b): $k = 0.7$, $\alpha = 1$, $\varepsilon = 0.05$, $\beta = 2/3$, and $d = 0.3$), (b); $\lambda' = -0.9$).

4. Numerical simulations and circuit experiments

The CNN with the feedback input $u(n)$ was implemented with the switched-capacitor circuit technique [8]. The circuit equations of the CNN circuit proposed in [7] are given by

$$\begin{aligned} V_{x1}(n+1) &= \left(1 - \frac{C_k}{C_i}\right)V_{x1}(n) - \frac{C_f}{C_i}V_{y1}(n) + \frac{C_a}{C_i}V_a \\ &\quad - \frac{C_{13}}{C_i}V_{y3}(n) - \frac{C_{12}}{C_i}V_{y2}(n) + \frac{C_u}{C_i}V_u(n), \quad (10) \\ V_{x2}(n+1) &= \left(1 - \frac{C_k}{C_i}\right)V_{x2}(n) - \frac{C_f}{C_i}V_{y2}(n) + \frac{C_a}{C_i}V_a \\ &\quad - \frac{C_{21}}{C_i}V_{y1}(n) - \frac{C_{23}}{C_i}V_{y3}(n) + \frac{C_u}{C_i}V_u(n), \quad (11) \\ V_{x3}(n+1) &= \left(1 - \frac{C_k}{C_i}\right)V_{x3}(n) - \frac{C_f}{C_i}V_{y3}(n) + \frac{C_a}{C_i}V_a \\ &\quad - \frac{C_{32}}{C_i}V_{y2}(n) - \frac{C_{31}}{C_i}V_{y1}(n) + \frac{C_u}{C_i}V_u(n). \quad (12) \end{aligned}$$

In the following simulations and experiments, we use the network parameters of $k = 0.7$, $\alpha = 1$, $\beta = 0.66$, $d = 0.2$, and $F = 0.26$. Note that these values are different from those used in [7]. In order to set these parameter values by the capacitor ratios in the circuit in [7], we used the capacitance values listed in Table 1.

Figure 2(a) shows the bifurcation diagram with a as a bifurcation parameter obtained from the numerical simulation without the feedback control. The bifurcation diagram changed with the feedback control as shown in Fig. 2(b). In the simulations, Gaussian noises were added considering the noises in the experiments.

On the other hand, the corresponding measured bifurcation diagrams obtained through the circuit experiments are shown in Fig. 3. That is, Fig. 3(a) shows the measured bifurcation diagram when we swept V_a without the feedback control, while that with the feedback control is shown in Fig. 3(b). In Figs. 3(a) and (b), the voltages V_a and $V_{x1}(n)$ were normalized by 4 V and 5 V, respectively, for easy comparison to the results in Figs. 2(a) and (b). From Figs. 2 and 3, we confirm the good agreement between the simulation and experiment results even with noise and device mismatches in the circuit.

Figure 4 shows phase-plane plots of $x_1(n)$ and $x_2(n)$ when (a) $a = -0.0625$, (b) $a = -0.03$, (c) $a = 0.125$, and (d) $a = 0.03$ obtained through numerical simulations. The corresponding measured phase-plane plots with (a) $V_a = -0.2$, (b) $V_a = -0.05$, (c) $V_a = 0.1$, and (d) $V_a = 0.2$

Table 1: Capacitance values.

C_i	470 pF
C_k	141 pF
C_a	470 pF
C_f	157 pF
C_{12}, C_{23}, C_{31}	110 pF
C_{13}, C_{21}, C_{32}	204 pF
C_u	122 pF

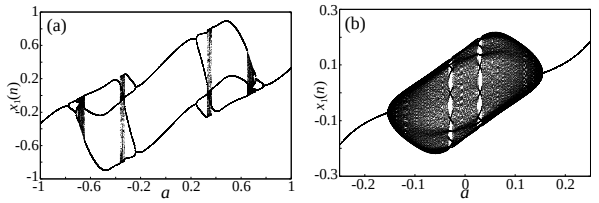

Figure 2: The simulated bifurcation diagrams of $x_1(n)$ when we change a, (a) without, and (b) with control.

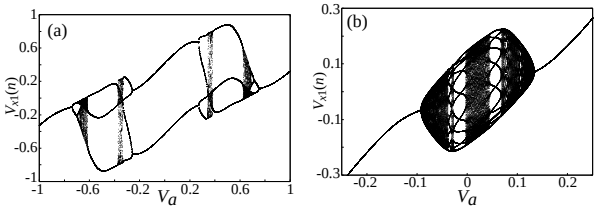

Figure 3: The measured bifurcation diagrams of $V_{x1}(n)$, (a) without, and (b) with the feedback control.

are shown in Fig. 5. Again in the figure, voltages $V_{x1}(n)$ and $V_{x2}(n)$ are normalized by 4 V. The attractors shown in Figs. 4(b) and (d), and Figs. 5(b) and (d) seem to be periodic solutions. In contrast, the attractors shown in Figs. 4(a) and (c), and Figs. 5(a) and (c) are the closed curves so that the solutions would be quasi-periodic.

The Lyapunov exponent is effective to distinguish the attractors. However, it is difficult to accurately calculate the Lyapunov exponents from the measured values because of noises. Therefore, we use the test method proposed by Ichinose [10] for quasi-periodic solution time-series for noisy experimental data.

5. The test method for quasi-periodic orbits

The test method utilizes the similarity between the random walk and the effect of dynamical noise on the quasi-periodic orbit in which the largest Lyapunov exponent is zero [10]. This method is also effective to test the noisy periodic orbit. In this test, whether a given time series is the random walk or not is determined based on the augmented Dickey-Fuller test. If p-value < 0.05, we can say the time series under test is not quasi-periodic.

We tested the attractors in Figs. 4 and 5, and the results are shown in Table 2. From Table 2, we find that the attractors of Figs. 4(a) and (c), and Figs. 5(a) and (c) are quasi-periodic solutions, while the attractors of Figs. 4(b) and (d), and Figs. 5(b) and (d) are the periodic solutions.

Table 2: Test results of the attractors.

Fig. 4 : Simulations		Fig. 5 : Circuit experiments	
Attractors	p-value	Attractors	p-value
(a)	0.4974	(a)	0.2042
(b)	0.01	(b)	0.01
(c)	0.6431	(c)	0.2974
(d)	0.01	(d)	0.01

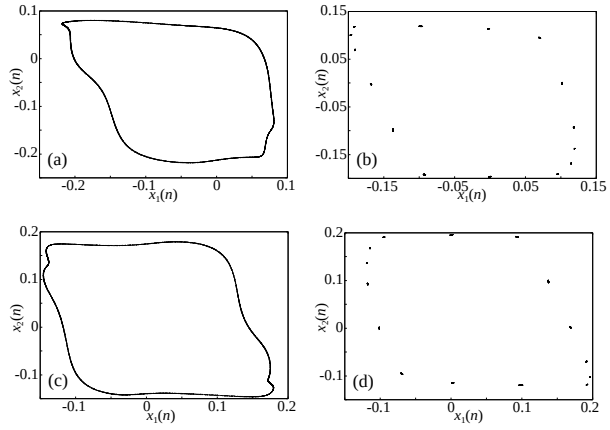

Figure 4: The phase-plane portrait of $x_1(n)$ and $x_2(n)$ obtained by the numerical simulation, (a) $a = -0.0625$, (b) $a = -0.03$, (c) $a = 0.125$, and (d) $a = 0.03$.

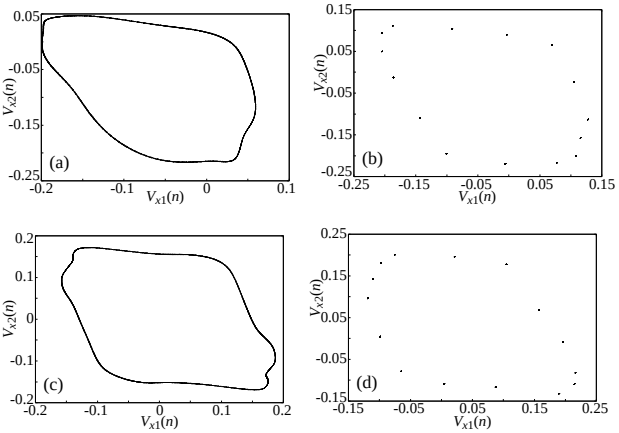

Figure 5: The measured phase-plane portrait of $V_{x1}(n)$ and $V_{x2}(n)$, (a) $V_a = -0.2$, (b) $V_a = -0.05$, (c) $V_a = 0.1$, and (d) $V_a = 0.2$.

6. The asymmetric CNN with 5 neurons

We extend the 3-neuron CNN to the 5-neuron CNN as

$$\begin{aligned} x_1(n+1) &= kx_1(n) - (\alpha-\beta)y_1(n) + a - \frac{\beta-d_1-d_2}{4}y_2(n) \\ &\quad -\frac{\beta-d_1+d_2}{4}y_3(n) - \frac{\beta+d_1-d_2}{4}y_4(n) \\ &\quad -\frac{\beta+d_1+d_2}{4}y_5(n) + F\cdot u(n), \end{aligned} \tag{13}$$

$$\begin{aligned} x_2(n+1) &= kx_2(n) - (\alpha-\beta)y_2(n) + a - \frac{\beta-d_1-d_2}{4}y_3(n) \\ &\quad -\frac{\beta-d_1+d_2}{4}y_4(n) - \frac{\beta+d_1-d_2}{4}y_5(n) \\ &\quad -\frac{\beta+d_1+d_2}{4}y_1(n) + F\cdot u(n), \end{aligned} \tag{14}$$

$$\begin{aligned} x_3(n+1) &= kx_3(n) - (\alpha-\beta)y_3(n) + a - \frac{\beta-d_1-d_2}{4}y_4(n) \\ &\quad -\frac{\beta-d_1+d_2}{4}y_5(n) - \frac{\beta+d_1-d_2}{4}y_1(n) \\ &\quad -\frac{\beta+d_1+d_2}{4}y_2(n) + F\cdot u(n), \end{aligned} \tag{15}$$

$$
\begin{aligned}
x_4(n+1) &= kx_4(n) - (\alpha-\beta)y_1(n) + a - \frac{\beta-d_1-d_2}{4}y_5(n) \\
&\quad -\frac{\beta-d_1+d_2}{4}y_1(n) - \frac{\beta+d_1-d_2}{4}y_2(n) \\
&\quad -\frac{\beta+d_1+d_2}{4}y_3(n) + F\cdot u(n), \qquad (16)\\
x_5(n+1) &= kx_5(n) - (\alpha-\beta)y_2(n) + a - \frac{\beta-d_1-d_2}{4}y_1(n) \\
&\quad -\frac{\beta-d_1+d_2}{4}y_2(n) - \frac{\beta+d_1-d_2}{4}y_3(n) \\
&\quad -\frac{\beta+d_1+d_2}{4}y_4(n) + F\cdot u(n), \qquad (17)
\end{aligned}
$$

where d_1 and d_2 enforce the asymmetric connection.

When the $u(n) = 0$, the eigenvalues of the Jacobian matrix J at the synchronized fixed point x^* can be given as

$$
\begin{aligned}
\lambda_1 &= k - \alpha\gamma, \\
\lambda_{2,3} &= k - \left(\alpha - \frac{5}{4}\beta\right)\gamma \\
&\quad \pm i\frac{\sqrt{(5d_1^2+5d_2^2)\gamma^2 + 2\sqrt{5}|(d_1^2+d_1d_2-d_2^2)\gamma^2|}}{4}, \\
\lambda_{4,5} &= k - \left(\alpha - \frac{5}{4}\beta\right)\gamma \\
&\quad \pm i\frac{\sqrt{(5d_1^2+5d_2^2)\gamma^2 - 2\sqrt{5}|(d_1^2+d_1d_2-d_2^2)\gamma^2|}}{4}. \qquad (18)
\end{aligned}
$$

The bifurcation diagrams of $x_1(n)$ obtained through numerical simulations are shown Figs. 6(a) and (b), without and with control, respectively. The parameter values used for these figures are: $k = 0.7$, $\alpha = 1$, $\beta = 0.66$, $d_1 = d_2 = 0.15$, and $F = 0.16$. These results show that the control procedure is applicable to the networks with 5 neurons.

7. Conclusion

We have experimentally demonstrated the stabilization of the unstable quasi-periodic orbit in the asymmetric 3-neuron CNN circuit constructed with the switched-capacitor circuit technique. The experimental results showed good agreements with those obtained from numerical simulations even with noise and device mismatches in the circuit. This confirms the robustness of the control method.

The obtained attractors have been tested through the test method dedicated to noisy time series. With this test, we distinguished the quasi-periodic and periodic orbits obtained from experiments.

We then have extended the 3-neuron CNN to the 5-neuron CNN. We apply the same control procedure to the 5-neuron asymmetric CNN as for the 3-neuron CNN to stabilize the quasi-periodic orbits. As a results of numerical simulations, we confirmed the effectiveness of the control method.

As a future problem, the quasi-periodic orbit in the 5-neuron CNN circuit will be experimentally stabilized. In addition, more general connection structure in the CNN will be used.

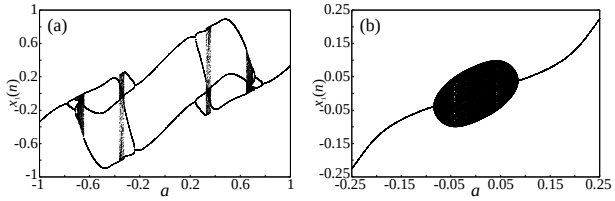

Figure 6: The simulated bifurcation diagrams of $x_1(n)$ when we change a, (a) without, and (b) with control.

References

[1] E. Ott, C. Grebogi, and J. A. Yorke, "Controlling chaos," Physical Review Letters, vol. 64, no. 11, pp. 1196–1199, 1990.

[2] K. Pyragas, "Continuous control of chaos by self-controlling feedback," Physics Letters A, vol. 170, pp. 421–428, 1992.

[3] N. Ichinose and M. Komuro, "Delayed feedback control and phase reduction of unstable quasi-periodic orbits," AIP Chaos, vol. 24, no. 3, 2014, DOI:10.1063/1.4896219.

[4] K. Kamiyama, M. Komuro, and T. Endo, "Algorithms for obtaining a saddle torus between two attractors," Int. J. Bifurcation and Chaos, vol. 23, no. 9, 2013, DOI:10.1142/S0218127413300322.

[5] N. Ichinose and M. Komuro, "Stabilization control of quasi-periodic orbits," in Analysis and Control of Complex Dynamical Systems, K. Aihara, J. Imura and T. Ueta eds., pp. 91–107, Springer Japan, 2015.

[6] K. Aihara, T. Takabe, and M. Toyoda, "Chaotic neural networks," Physics Letters A, vol. 144, pp. 333–340, 1990.

[7] M. Ogawa, Y. Horio, N. Ichinose and M. Komuro, "Circuit experiments on stabilization of unstable quasi-periodic solutions in an asymmetric chaotic neural network circuit," in Proc. IEICE The 28th Workshop on Circuits and Systems, pp. 136–141, 2015 (in Japanese).

[8] Y. Horio and K. Suyama, "Switched-capacitor chaotic neuron for chaotic neural networks," in Proc. IEEE Int. Symp. on Circuits and Syst., vol. 2, pp. 1018–1021, 1993.

[9] W. M. Wonham, "On pole assignment in multi-input controllable linear systems," IEEE Trans. Autom. Control, vol. AC–12, no. 6, 1967, DOI:10.1109/TAC.1967.1098739.

[10] N. Ichinose, "Time series test for noisy quasi-periodic solution," Technical Note, 2015 (in Japanese).